Melting Behavior and Isothermal Crystallization Kinetics of Polypropylene/Metallocene-Catalyzed Polyethylene Elastomer Blends

ARTICLE *in* JOURNAL OF APPLIED POLYMER SCIENCE · DECEMBER 2008

Impact Factor: 1.77 · DOI: 10.1002/app.28783

3 AUTHORS, INCLUDING:

Jianglei Qin
Hebei University
19 PUBLICATIONS **121** CITATIONS

Melting Behavior and Isothermal Crystallization Kinetics of Polypropylene/Metallocene-Catalyzed Polyethylene Elastomer Blends

Jianglei Qin, Shiqi Zhang, Zhiting Li

College of Chemistry and Environmental Science, Hebei University, Baoding 071002, China

Received 23 July 2007; accepted 28 May 2008
DOI 10.1002/app.28783
Published online 22 August 2008 in Wiley InterScience (www.interscience.wiley.com).

ABSTRACT: Polypropylene (PP)/metallocene-catalyzed polyethylene elastomer (mPE) blends were prepared in a twin-screw extruder. The melting behavior, crystallization behavior, and isothermal crystallization kinetics of the blends were studied with differential scanning calorimetry. The results showed that PP and mPE were partially miscible and that the addition of mPE shifted the melting peak of PP to a lower temperature but the crystallization temperature to a higher temperature, demonstrating a dilution effect of mPE on PP. The isothermal crystallization kinetics of the blends were described with the Avrami equation. The values of the Avrami exponent indicated that the nucleation mechanism of the blends was heterogeneous, the growth of spherulites was almost three-dimensional, and the crystallization mechanism of PP was not affected much by mPE. At the same time, the Avrami exponents of the blends were higher than that of pure PP, and this showed that the addition of mPE helped PP to form more perfect spherulites. The crystallization rate of PP was increased by mPE because the dilution effect of mPE on PP increased the mobility of PP chains. The crystallization activation energy was estimated with the Arrhenius equation, and the nucleation constant was determined by the Hoffman–Lauritzen theory. © 2008 Wiley Periodicals, Inc. J Appl Polym Sci 110: 2615–2622, 2008

Key words: activation energy; blends; crystallization; melt; metallocene catalysts

INTRODUCTION

Polypropylene (PP) is a semicrystalline thermoplastic polymeric material that is widely used because of its attractive combination of good processability, good mechanical properties, good chemical resistance, and a low price. However, its application in some fields is limited by its low fracture toughness at low temperatures and high notch sensitivity at room temperature. To improve the impact properties of PP, blending PP with a dispersed elastomeric phase (e.g., polypropylene random, ethylene-propylene rubber, styrene-ethylene-butadiene-styrene, ethylene propylene diene monomer) is widely practiced[1–7] because the elastomer can increase the overall toughness of the PP matrix.[8] However, the addition of an elastomer often has negative effects on some properties of PP, such as stiffness and hardness.[9]

The development of metallocene catalysts has led to the production of numerous new polyolefin materials in both elastomeric and nonelastomeric fields, and the crystallization behavior of metallocene-catalyzed polyethylene is obviously different from that of Ziegler–Natta polyethylene; this also differs in the branching characteristics and copolymer composition distribution.[10] Among these, metallocene-catalyzed polyolefin elastomers are extremely attractive in both rubber and plastic industries. A metallocene-catalyzed polyethylene elastomer (mPE) polymerized with octene as a comonomer possesses a very homogeneous copolymer distribution and a narrow molecular mass distribution. Because of its good thermal stability, good mechanical properties, and good puncture strength in comparison with conventional rubber modifiers, mPE can impart higher impact strength to PP; at the same time, its good processability and tensile strength are well maintained.[9] In addition, previous work has shown improved fracture behavior at low temperatures and better dynamic properties of PP with mPE as a modifier.[11] Also, mPE exists in a granular form, so its processing technology (e.g., extrusion and injection molding) during blending with PP is very convenient.

It is well known that the physical properties of semicrystalline polymeric materials strongly depend on their crystallization and microstructure, so an investigation of the crystallization behavior is significant both theoretically and practically. Therefore, it is highly desirable to investigate the crystallization

Correspondence to: J. Qin (thunder20@163.com).
Contract grant sponsor: Science Foundation of Hebei University; contract grant number: 2006Q13.

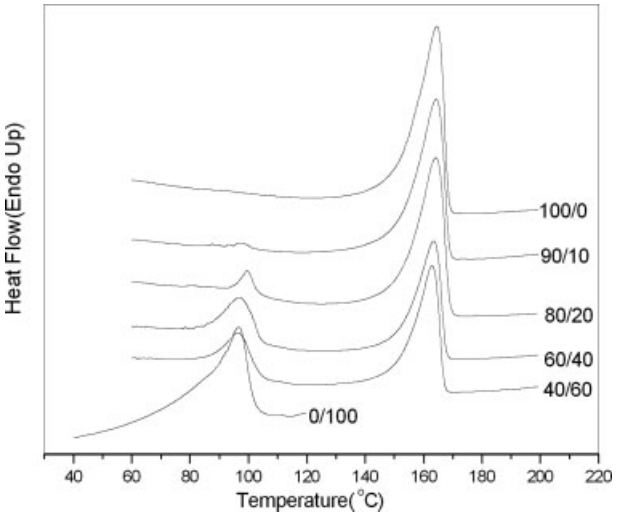

Figure 1 DSC melting curves of PP/mPE blends at a heating rate of 10°C/min.

kinetics to optimize their blend composition and understand the properties of the processed products. The nonisothermal crystallization kinetics of PP/mPE blends have been reported,[12] but the isothermal crystallization kinetics, which can provide the Avrami exponent (n) showing the growing patterns and nucleation mechanism of the spherulites, have not been reported yet.

In this study, the melting behavior and isothermal crystallization kinetics of PP/mPE blends were investigated intensively, and Avrami analysis was applied to them to investigate the isothermal crystallization kinetics and nucleation mechanism. The activation energy (E_a) was calculated with an Arrhenius equation, and the nucleation constant (K_g) was determined with the Hoffman–Lauritzen theory.

EXPERIMENTAL

Materials

The PP [type T36F, density (d) = 0.91 g/cm^3, melt flow index (230°C/2.16 kg) = 2.4 g/10 min] used in this study was supplied by Qilu Petrochemical Co. (China). The mPE sample [type 0201C-8, d = 0.895 g/cm^3, melt flow index (190°C/2.16 kg) = 0.93 g/10 min] was obtained from Qatar Petrochemical Co. All of the materials were used as received.

Preparation of the PP/mPE blends

The blending process was carried out in a corotational twin-screw extruder with a length/diameter ratio of 28 (TE-34, Coperion Keya, Nanjing, China), and the temperature of the barrel was set around 220°C. The weight ratios of PP to mPE in the blends were 100/0, 90/10, 80/20, 60/40, 40/60, and 0/100.

Characterization

A differential scanning calorimeter (PerkinElmer, DSC-7) equipped with an intracooling unit was used to record the heat flow of the heating processes, cooling processes, and isothermal crystallization kinetics of the blends. All of the operations were carried out under a nitrogen environment. The temperature and melting enthalpy were calibrated with standard indium. To minimize thermal lag between the polymer sample and the differential scanning calorimetry (DSC) furnace, all sample weights were set at about 9 mg.

To determine the melting and crystallization behaviors, the samples were heated from room temperature to 200°C at a rate of 10°C/min; to erase the thermal history, the temperature was held at 200°C for 1 min and then cooled to 50°C at a rate of 10°C/min. To determine the isothermal crystallization kinetics, samples were heated from room temperature to 200°C, maintained at that temperature for 1 min, then cooled to the required crystallization temperature (T_c = 122–128°C) at a cooling rate of 150°C/min, and held for 30 min to record the heat flow. The half-time of isothermal crystallization ($t_{1/2}$) was defined as the time needed for 50% crystallization.

RESULTS AND DISCUSSION

Melting and crystallization behaviors of the PP/mPE blends

The melting heat flows of the pure polymers and their blends are shown in Figure 1. The melting temperature of PP (T_{m2}) decreased with increasing mPE content (see Table I); however, the melting temperature of mPE (T_{m1}) increased with increasing PP content. The melting peaks of PP were between 163.0 and 164.4°C, which indicated that PP, both in the pure state and in the blends, exhibited only α crystals.[13,14] The changes in T_{m2} and T_{m1} were not obvious because the miscibility of the two components was limited.

TABLE I
T_m and T_c Values of the PP/mPE Blends

Sample (PP/mPE)	T_{m1} (°C)	T_{m2} (°C)	T_{c1} (°C)	T_{c2} (°C)
100/0	—	164.4	111.0	—
90/10	99.3	164.4	112.2	—
80/20	99.7	164.0	112.2	84.8
60/40	97.0	163.4	115.7	83.3
40/60	96.6	163.0	115.0	83.3
0/100	96.6	—	—	83.0

Both the heating and cooling rates were 10°C/min.

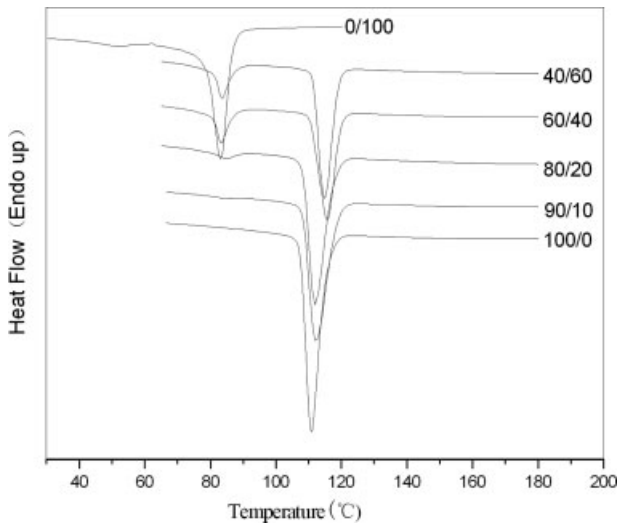

Figure 2 DSC cooling curves of PP/mPE blends at a cooling rate of 10°C/min.

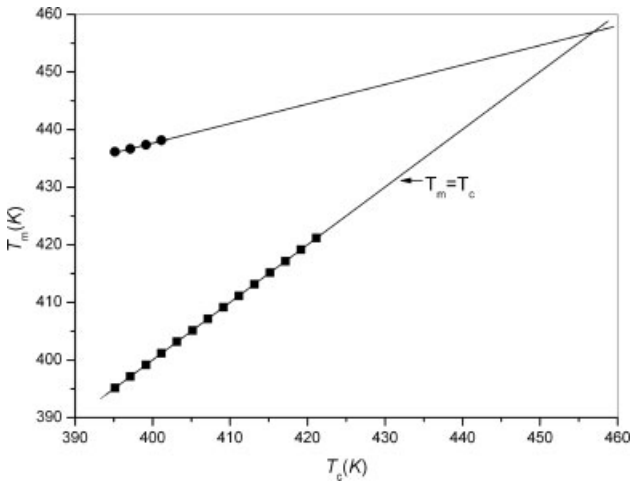

Figure 3 Hoffman–Weeks plots for the determination of T_m^0 for PP/mPE (82/20) blends.

For the pure PP, pure mPE, and their blends, which were crystallizable, the nonisothermal crystallization behaviors were also measured in the molten state by DSC with a cooling rate of 10°C/min. Figure 2 shows the crystallization exotherms for some PP/mPE blends compared to the pure polymer. All of the DSC traces showed two crystallization peaks, except that of the pure polymers, which indicated that these systems existed as two crystallizable components. The exotherm peak of mPE was 83.0°C, and the exotherm peak of PP was 111.0°C. The melting temperatures (T_m) and T_c's of the blends systems are listed in Table I. The T_c of mPE increased with increasing PP content; however, the T_c of PP increased with increasing mPE content. This indicated the mPE had some dilution effect on PP. Compared to the Ziegler–Natta polyethylene, mPE is a kind of elastomer, and the T_c is low,[15] but in contrast to EPR, mPE can crystallize.[16]

This observation was further confirmed by the measurement of the equilibrium melting points (T_m^0's). Shown in Figure 3 are the plots of the apparent melting temperature (T_m') as a function of T_c for the 80/20 PP/mPE blends for a wide range of undercooling. The T_m^0 values were determined by extrapolation to the lines of T_m' to T_c according to the Hoffman–Weeks equation:[17]

$$T_m' = \varphi T_c + (1 - \varphi)T_m^0 \quad (1)$$

where φ is a stability parameter. The value of φ is between 0 and 1. The φ parameters could be obtained from the slope of the straight lines, and the values of T_m^0 were determined by extrapolation of the least squares fit lines of the experimental data according to eq. (1) to intersect the line where $T_m = T_c$, as shown in Figure 3. T_m^0 and φ are listed in Table II. The φ value was 0.37 for pure PP and 0.34 for the blends. In terms of φ, we judged that the spherulites in pure PP were more stable than those in the blends because some mPE chains entered the PP spherulites; this was proven by the increasing crystallinity of PP with the addition of mPE. At the same time, the T_m^0 values of the PP/mPE blends were lower than that of pure PP because of the lower stability of the PP spherulites in the blends.

The isothermal crystallization behaviors of the PP/mPE blends were studied by DSC. Figure 4 shows the DSC heat flows of PP and PP/mPE blends that were isothermally crystallized at different temperatures. The chosen T_c values were determined through a series of experiments conducted at various T_c values. As shown in Figure 4, the shape of the exotherm peaks were similar, but the peak time (t_p) decreased with increasing mPE content; this was consistent with a former conclusion that the T_c increased with increasing mPE content. The t_p values are listed in Table II. For a given sample, the exothermal peak shifted to longer times, and t_p increased with increasing T_c, which showed that the higher supercooling was, the higher the crystallization rate was and that crystallization was enhanced as the temperature decreased.

TABLE II
T_m^0, $\ln[1/(t_{1/2})_0]$, and K_g Values of PP/mPE Blends Calculated with the Lauritzen–Hoffman Equation

Sample (PP/mPE)	T_m^0 (K)	φ	K_g (K^2)	σ_e (mJ/m^2)	$\ln[1/(t_{1/2})_0]$
100/0	458.8	0.37	5.06×10^5	108.1	25.80
80/20	456.8	0.34	5.83×10^5	125.1	29.76
60/40	455.9	0.34	5.80×10^5	124.7	30.13

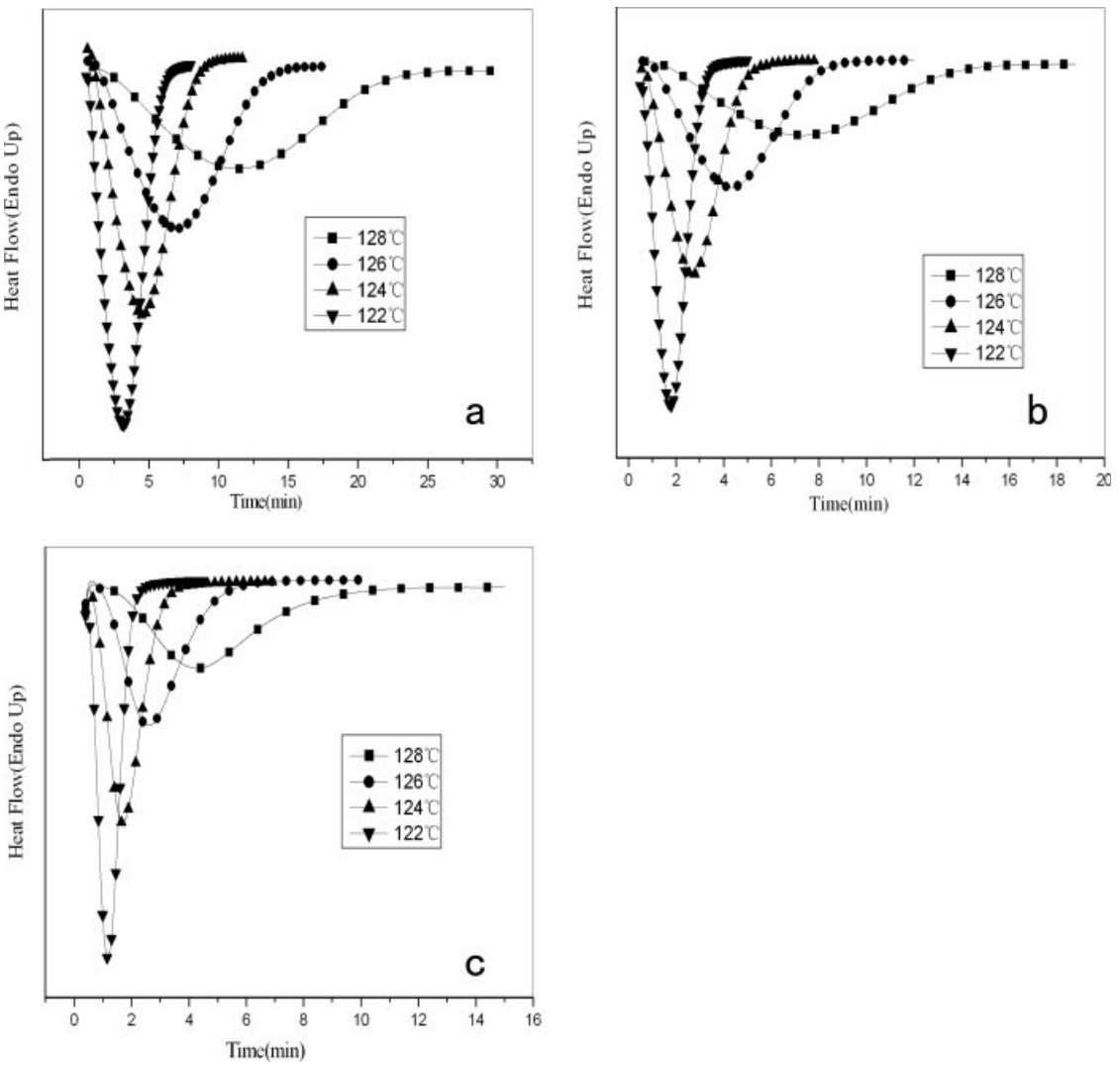

Figure 4 DSC isothermal crystallization curves for PP/mPE blends at various T_c values: (a) 100/0, (b) 80/20, and (c) 60/40.

Isothermal crystallization kinetics

The Avrami equation[18,19] has been widely used to describe isothermal crystallization kinetics[20–22] and has been modified to describe the nonisothermal crystallization kinetics of polymers:[21–26]

$$1 - X_t = \exp(-kt^n) \tag{2}$$

where X_t is the relative crystallinity, k is the growth rate constant, t is the crystallization time, and n is the Avrami exponent. Here, the value of n depends on the nucleation mechanism and growth dimension. A value of $n = 4$ shows that the nucleation mechanism is homogeneous, and a value of $n = 3$ shows that the nucleation mechanism is heterogeneous.

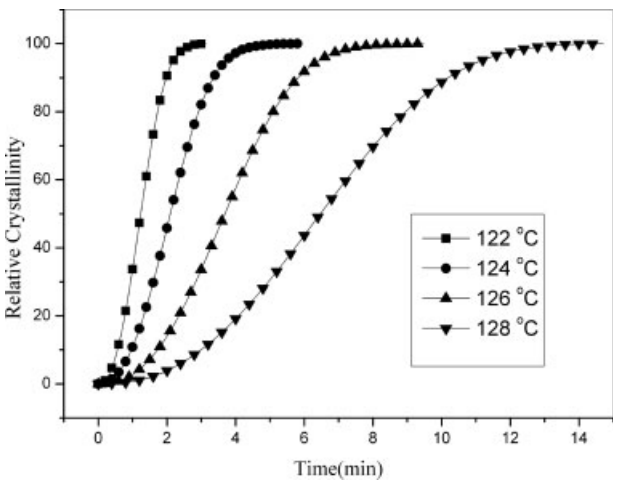

Figure 5 Plot of X_t versus t for the isothermal crystallization of PP/mPE (80/20) blends at various T_c values.

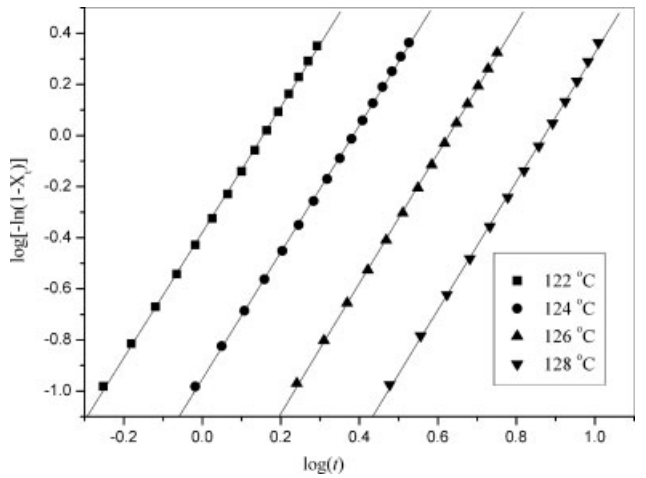

Figure 6 Avrami plot for the isothermal crystallization of PP/mPE (80/20) blends at various T_c values.

X_t versus t for the 80/20 PP/mPE blends at various T_c's is shown in Figure 5. All of the curves in Figure 5 showed a sigmoidal shape, which indicated a fast primary crystallization process during the initial stages and a slower secondary crystallization process during the later stages. The plot of X_t versus t shifted to the right when T_c increased, which showed a decrease in the crystallization rate and indicated that the crystallization rate was enhanced as the temperature decreased. That was because of the strong temperature dependence of the nucleation and the growth parameters.[27] After the maximum in the heat flow curves passed, a small fraction of crystallinity developed by slower, secondary kinetics processes.

With the relative degree of crystallinity assumed to increase with increasing t, the Avrami equation can be rewritten in a double-logarithm form:

$$\log[-\ln(1 - X_t)] = \log\ k + n \log\ t \qquad (3)$$

where the Avrami exponent n is a constant that depends on the type of nucleation and growth of the crystals and k is a crystallization rate constant involving both nucleation and growth rate parameters under isothermal conditions. Usually, the values of n should be an integer between 1 and 4 for different crystallization mechanisms. Because other complex factors, such as the competition of a diffusion-controlled growth and/or the irregular boundary of the spherulites, are probably involved in the process, n is not a straight forward integer.[28] By plotting $\log[-\ln(1 - X_t)]$ versus $\log t$, we obtained n and $\log k$ from the slope and intercept, respectively; the $\log[-\ln(1 - X_t)]$ versus $\log t$ plots of 80/20 PP/mPE are shown in Figure 6. Each curve showed a good linear relationship, which indicated that the Avrami equation properly described the isothermal crystallization kinetics of these blends systems. The X_t ranges were from 10 to 90%, which showed good fitness of the Avrami equation to these systems in the whole process. Similar shapes and trends appeared in pure PP and the 60/40 PP/mPE blends.

As shown, all of the lines in Figure 6 are almost paralleled to each other, shifting to lower times with decreasing T_c. This implies that the nucleation mechanism and crystal growth geometries were similar, although the T_c's were different. n and the crystallization rate constant were estimated from the slope and intercept of the $\ln[-\ln(1 - X_t)]$ versus $\ln t$ plot, and the values are listed in Table III. Regardless of the T_c values, the n values for pure PP were between 2.33 and 2.56; compared to literature data under isothermal conditions,[29,30] this indicated that heterogeneous nucleation and the growth of spherulites were between two dimensional and three dimensional. The n values for the PP/mPE blends were in the range 2.46–2.65, which was a little higher than that of pure PP. These results show that mPE helped PP to form more perfect spherulites. The $\log k$ (crystallization rate constant) values of the blends were larger than that of pure PP, which indicated that the mPE increased the crystallization rate of PP. This was because the dilution effect of mPE helped the PP chains to transit to the growing crystal.

The mechanism of mPE on the crystallization kinetics of PP was that, at the T_c's, because of the high supercooling, the mobility of the PP chains was not high enough to transit from the amorphous state to the growing crystal, and the spherulites are not perfect. However, at that temperature, mPE was unable to crystallize, and the mobility of the mPE chains was still high. At the same time, the partial miscibility and interaction of PP and mPE led to a small part of the PP chains dissolving into the mPE melt. The mobility of the dissolved PP chains was much higher than that of the pure PP, and then, the PP chains could transit to the growing crystal and

TABLE III
Isothermal Crystallization Parameters of the PP/mPE Blends at Different T_c Values

Sample (PP/mPE)	T_c (°C)	$t_{1/2}$ (min)	n	$\log k$	t_p (min)
100/0	122	2.62	2.33	2.57	−1.12
	124	3.88	2.47	−1.60	3.78
	126	6.40	2.56	−2.22	6.30
	128	10.6	2.52	−2.75	10.5
80/20	122	1.24	2.46	−0.38	1.20
	124	2.10	2.48	−0.95	2.04
	126	3.69	2.55	−1.60	3.58
	128	6.48	2.51	−2.19	6.34
60/40	122	0.74	2.54	0.16	0.67
	124	1.28	2.65	−0.45	1.18
	126	2.21	2.65	−1.09	2.00
	128	3.85	2.59	−1.69	3.45

T_c, crystallization temperature.

form perfect spherulites through the mPE melt. Because the mPE could not form solid nuclei at T_c, the nucleation mechanism of PP was not obviously affected.

However, the crystallization rate was dependent on the blend composition and T_c. On one hand, for all of the samples, the crystallization rate constant (k) increased with decreasing T_c, whereas $t_{1/2}$ decreased with decreasing T_c (see Table III). On the other hand, both k and $t_{1/2}$ were also influenced by the addition of mPE. That is, at the same T_c, k increased slightly with increasing mPE content, and $t_{1/2}$ was adversely affected. Thus, the crystallization rate accelerated with increasing mPE content in PP, which was due to the dilution effect of mPE on PP, which shifted the crystallization point of PP to a higher temperature. So at the same T_c, the supercooling of PP was then increased by addition of mPE, and the crystallization rates were enhanced by the high supercooling. So at T_c, the miscibility of PP and mPE favored an improvement in the mobility of the PP molecules; then, the crystallization rate increased, and the spherulites became more perfect with the addition of mPE in the PP/mPE blends.

$t_{1/2}$ is a very important parameter, which is defined as the time from the onset of the crystallization until 50% completion. The $t_{1/2}$ values can always be drawn directly from the X_t versus time plot, as shown in Table III; t_p values are also shown for comparison. As shown in Table III, the t_p values were near but a little lower than that of $t_{1/2}$. This was because of the secondary crystallization of PP, and then, the X_t values were lower than 50% when the crystallization rate reached its highest.

Also, $t_{1/2}$ could be determined from the measured kinetics parameters, as follows:[31]

$$t_{1/2} = \left(\frac{\ln 2}{k}\right)^{1/n} \tag{4}$$

The $t_{1/2}$ values drawn from the crystallinity versus time plot and calculated from eq. (4) are listed in Table IV for comparison, and the values were very close, which showed good consistency in the theoretical and experimental conclusions.

For all of the samples, the crystallinity of PP (X_{PP}) was defined as

$$X_{PP} = \frac{\Delta H_c}{187.7 \times PP\%} \tag{5}$$

where 187.7 (J/g) is the 100% crystallization enthalpy of PP[32] and ΔH_c is the crystallization enthalpy of PP in the pure PP or the PP/mPE blends. The X_{PP} values are also listed in Table IV. X_{PP} of 80/20 PP/mPE was higher than that of pure PP, which meant that the mPE chains entered the PP crystals.

TABLE IV
Comparison of the $t_{1/2}$ and Crystallinity Values of the Blends at Different T_c Values

Sample (PP/mPE)	T_c (°C)	Experimental (min)	Calculated from k (min)	X_{PP} (%)
100/0	122	2.62	2.58	43.4
	124	3.88	3.83	45.6
	126	6.40	6.38	46.0
	128	10.6	10.67	46.9
80/20	122	1.24	1.23	44.6
	124	2.10	2.08	47.6
	126	3.69	3.67	49.7
	128	6.48	6.44	50.0
60/40	122	0.74	0.75	41.2
	124	1.28	1.29	44.1
	126	2.21	2.25	46.3
	128	3.85	3.90	47.0

This was more proof of the partial miscibility of PP and mPE. However, the X_{PP} of 60/40 PP/mPE was lower than that of the 80/20 PP/mPE blends because part of the PP dissolved into the mPE and was unable to crystallize at that temperature. The crystallinity of the both PP and the PP/mPE blends increased with increasing of T_c, and this result indicates that the mobility of the PP chains increased with increasing temperature, and then, the crystallinity was correspondingly higher.

The Avrami parameter (k) was assumed to be thermally activated and was used to determine the E_a for crystallization. Thus, the crystallization rate parameter (k) could be described by an Arrhenius relation[33] as follows:

$$k^{1/n} = k_0 \exp\left(-\frac{E_a}{RT_c}\right) \tag{6}$$

where k_0 is a temperature-independent pre-exponential factor, E_a is the activation energy, R is the gas constant, and T_c is the crystallization temperature. E_a/R was determined by the linear regression of the experimental data $\ln k^{-1/n}$ versus $1/T$, as shown in Figure 7. The E_a of PP was −310.0 kJ/mol; at the same time, the E_a values of the 80/20 PP/mPE and 60/40 PP/mPE blends were −364.0 and −362.4 kJ/mol, respectively. These results show that the crystallization energy of the PP/mPE blends was lower than that of pure PP and that the crystallization rate was correspondingly higher. On the other hand, the crystallization rate of the PP/mPE blends was more sensitive to temperature than that of pure PP. This conclusion was consistent with the Avrami analysis.

To further investigate the crystal growth kinetics of PP and the blends isothermally crystallized from the melt, the Lauritzen–Hoffman equation[34] was applied in this study to analyze the spherulite growth rate of the system. On the basis of this theory, the crystal growth rate (G) at a given T_c is expressed by the following equation.

$$G = G_0 \exp\left[-\frac{U^*}{R(T_c - T_\infty)}\right] \exp\left[-\frac{K_g}{T_c(\Delta T)f}\right] \quad (7)$$

where G_0 is a pre-exponential factor, U^* is the activation energy for transporting the polymer chain segments to the crystallization site, R is the gas constant, T_∞ is the temperature below which the polymer chain movement ceases, ΔT is the degree of supercooling described as $T_c - T_m^0$, f is a correction factor accounting for the variation in the enthalpy of fusion (ΔH_f) given as $f = 2T_c/(T_m^0 + T_c)$, and K_g is the nucleation constant. In the experimental temperature range, K_g can be expressed as

$$K_g = 4b_0\sigma\sigma_e T_m^0/k_b(\Delta H_f) \quad (8)$$

where σ and σ_e are the free energies per unit area of the surfaces of the lamellae parallel and perpendicular, respectively, to the chain direction; b_0 is the distance between two adjacent fold planes; and k_b is the Boltzmann constant and is equal to 1.35×10^{-23} J mol^{-1} K^{-1}.

For practical convenience, $1/t_{1/2}$ and $(1/t_{1/2})_0$ were used to substitute for G and G_0 in the calculation. According to Chan and Isayev,[35] eq. (7) is usually rewritten as follows.

$$\ln\left(\frac{1}{t_{1/2}}\right) + \frac{U^*}{R(T_c - T_\infty)} = \ln\left[\left(\frac{1}{t_{1/2}}\right)_0\right] - \frac{K_g}{T_c(\Delta T)f} \quad (9)$$

In this study, universal values of $U^* = 6300$ or 1500 cal/mol and $T_\infty = T_g - 30$ K were used in all calculations.[34] The plot of $\ln(t_{1/2}) + U^*/R(T_c - T_\infty)$ versus $1/T_c\Delta Tf$ of the PP/mPE blends for isothermal crystallization are shown in Figure 8, and the straight line suggested the existence of only one crystallization regime. The values of K_g and $\ln[1/(t_{1/2})_0]$ were obtained from the slope and the intercept of Figure 8, and the values are listed in Table II. Also, σ_e was calculated by the substitution of K_g into eq. (8); with the assumption of crystal growth on the 110 plane, the values of σ, ΔH_f, and b_0 were 11.5 mJ/m^2, 209 J/g, and 62.6 nm,[36] respectively (see Table II). The K_g values of the PP/mPE blends were higher than that of pure PP, as were the σ_e values. The lower value of σ_e showed a nucleation effect, so the mPE did not act as nucleation agent in the blend systems. This result was consistent with the higher n of the blends than that of pure PP.

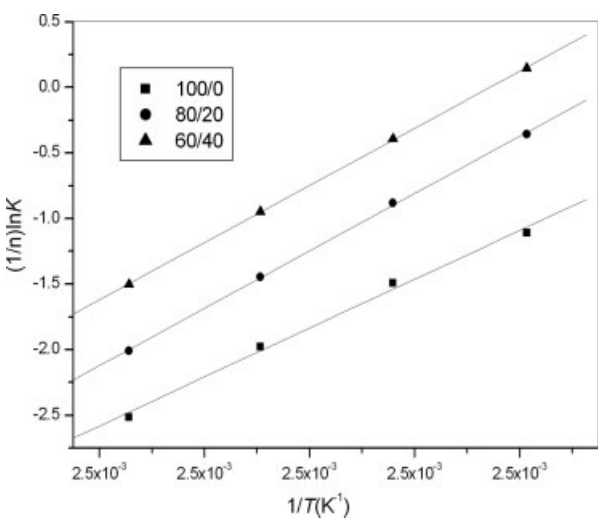

Figure 7 $(1/n)\ln K$ vs $1/T$ for evaluating E_a for isothermal crystallization.

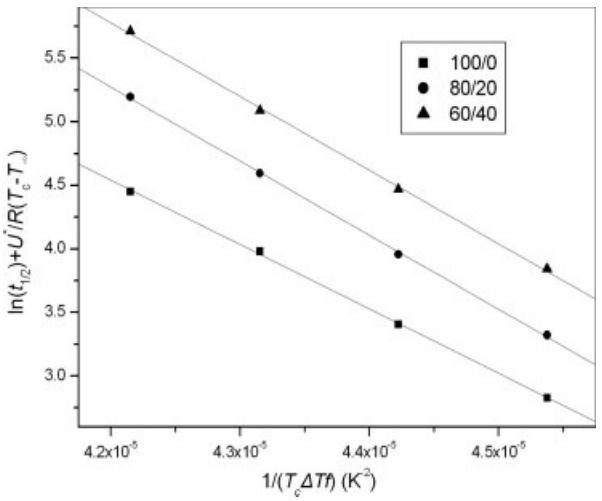

Figure 8 Plot of $\ln(t_{1/2}) + U^*/R(T_c - T_\infty)$ versus $1/T_c\Delta Tf$ for the isothermal crystallization of PP/mPE blends at different mPE contents.

CONCLUSIONS

PP/mPE blends prepared by the conventional melt-blending method were investigated for their melting and crystallization behaviors and isothermal crystallization kinetics:

1. The study of the melting and crystallization behaviors showed that the mPE had some dilution effect on PP. The crystallinity of PP increased with the addition of mPE, which showed that the mPE chains entered the PP matrix.
2. The isothermal crystallization kinetics of the blends were investigated fairly well with Avrami analysis. The values of n indicated that the crystallization nucleation mechanism was heterogeneous and that mPE did not affect the nucleation mechanism but helped PP to form more perfect spherulites.
3. E_a decreased and the crystallization rate increased with increasing content of mPE in the blends, which showed that mPE accelerated the overall crystallization processes.

References

1. Qiu, G.-X.; Raue, F.; Gottfried, W. J Appl Polym Sci 2002, 83, 3029.
2. Naiki, M.; Matsumura, T.; Matsuda, M. J Appl Polym Sci 2002, 83, 46.
3. Bassani, A.; Pessan, L. A. J Appl Polym Sci 2003, 88, 1081.
4. Coco-Pola, F.; Greco, R.; Martuscelli, E.; Kammer, H. W. Polymer 1987, 28, 47.
5. Tam, W. Y.; Cheung, T.; Li, R. K. Y. Polym Test 1996, 15, 452.
6. Van der Wal, A.; Mulder, J. J.; Oderkerk, J.; Gaymans, R. J. Polymer 1998, 39, 6781.
7. Bai, S.-L.; G'Sell, C.; Hiver, J.-M. Polymer 2005, 46, 6437.
8. Karger-Kocsis, J. Polypropylene—Structure, Blends and Composites; Chapman & Hall: London, 1994.
9. Qiu, G. X.; Raue, F.; Ehrenstein, G. W. J Appl Polym Sci 2002, 83, 3029.
10. Islam, M. A.; Hussein, I. A.; Atiqullah, M. Eur Polym J 2007, 43, 599.
11. Raue, F.; Ehrenstein, G. W. J Elast Plast 1998, 31, 194.
12. Gao, J.; Wang, D.; Yu, M. J Appl Polym Sci 2004, 93, 1203.
13. Shieh, Y. T.; Lee, M. S.; Chen, S. A. Polymer 2001, 42, 4439.
14. Ha, C. S.; Kim, S. C. J Appl Polym Sci 1988, 35, 2211.
15. Li, J.; Shanks, R. A.; Long, Y. J Appl Polym Sci 2001, 82, 628.
16. Yazdani-Pedram, M.; Quijada, R.; Lopez-Manchado, M. A. Macromol Mater Eng 2003, 11, 288.
17. Hoffman, J. D.; Weeks, J. J. J Chem Phys 1962, 37, 1723.
18. Avrami, M. J Chem Phys 1939, 7, 1103.
19. Avrami, M. J Chem Phys 1940, 8, 212.
20. Lu, X. L.; Hay, J. N. Polymer 2001, 42, 9423.
21. Li, J.; Zhou, C.; Wang, G. Polym Test 2002, 21, 583.
22. Run, M.; Yao, C.; Wang, Y. Eur Polym J 2006, 42, 655.
23. Ozawa, T. Polymer 1971, 12, 150.
24. Ozawa, T. Polymer 1978, 19, 1142.
25. Herrero, C. H.; Acosta, J. L. Polymer 1994, 26, 786.
26. Lee, S. W.; Ree, M.; Park, C. E.; Jung, Y. K.; Park, C. S.; Jin, Y. S.; Bae, D. C. Polymer 1999, 40, 7137.
27. Seo, Y. S.; Kim, J. H.; Kin, K. U.; Kim, Y. C. Polymer 2000, 41, 2639.
28. Shultz, J. Polymeric Materials Science; Prentice-Hall: New York, 1974.
29. Xu, G.; Shi, W.; Hu, P. Eur Polym J 2005, 41, 1828.
30. Li, J.; Zhou, C.; Wang, G.; Tao, Y. Polym Test 2002, 21, 583.
31. Zhang, X.; Xie, T.; Yang, G. Polymer 2006, 47, 2116.
32. Kirshenbaum, I.; Wilchinsky, Z. W.; Groten, B. J Appl Polym Sci 1964, 8, 2723.
33. Li, J.; Zhou, C.; Wang, G. Polym Test 2002, 21, 583.
34. Hoffman, J. D.; Davis, G. T.; Lauritzen, J. I., Jr. In Treatise on Solid State Chemistry; Hannay, N. B., Ed.; Plenum: New York, 1976; Vol. 3.
35. Chan, T. W.; Isayev, A. I. Polym Eng Sci 1994, 34, 461.
36. Clark, E. J.; Hoffman, J. D. Macromolecules 1984, 17, 878.